DYNAMIC FRACTURE SURFACE ENERGY VALUES AND FRUSTRATED MICRO-BRANCHES DURING RCP IN AN IMPACT MODIFIED POLYMER

C. Fond and R. Schirrer

Institut Charles Sadron, 6, rue Boussingault, F67083 Strasbourg.
fond@ics.u-strasbg.fr, schirrer.ics.u-strasbg.fr, http://ics.u-strasbg.fr/

ABSTRACT

The fracture behaviour of materials for which the fracture energy decreases near the Raleigh wave speed, c_r, is investigated using an impact modified polymer. An experimental device based on strip band geometry has been designed to explore the brittle behaviour of such polymers during rapid crack propagation (RCP). The macroscopic crack speed is found to be quasi-constant along an entire rubber toughened polymethylmethacrylate (RT-PMMA) specimen, even in the case of crack branching and until arrest, if any. As the material behaviour tends to accelerate the crack – the fracture energy decreases near c_r - whereas mechanical inertial effects tend to limit the rate of crack propagation – due to crack branching -, the macroscopic crack speed stabilizes at approximately $å_{mb} = 0.6\ c_r$, which is the macroscopic crack branching speed for RT-PMMA. Consequently, at the macroscopic crack branching velocity, the experimental fracture surface energy and the fracture surface roughness have no single value in such materials. In fact, the macroscopic fracture surface energy value increases with the number of instabilities or frustrated micro-branches.

INTRODUCTION

While the dynamic fracture behaviour of materials for which the fracture energy increases near the Raleigh wave speed, c_r, has been largely explored and is now relatively well understood – the speed of the cracks decrease at crack branching – the case of materials for which the fracture energy decreases near c_r is still to be investigated on real materials. Most polymeric materials exhibit a brittle fracture mode at high crack propagation speeds and experiments have revealed that crack propagation in rubber toughened-polymethylmethacrylate (RT-PMMA) is unstable between approximately 0.001 and 0.6 c_r, where c_r is the Raleigh wave speed. As the fracture surface energy decreases with increasing crack speed, the propagation velocity jumps from 1 to about 600 m/s when an increasing load initiates propagation of a crack. Crack branching occurs, as expected, at a crack tip speed of nearly 0.6 c_r. However, unlike in many other polymers such as for instance PMMA, the macroscopic crack speed ($å_m$) does not change after branching during rapid crack propagation (RCP) in RT-PMMA. In fact, at nearly 0.6 c_r, inertial effects modify the crack tip stress field and induce branching [1]. It is noticeable that branching is made easier by the rubber toughening particles, which perturb the micro-mechanical fields. Subsequently, as the material behaviour tends to accelerate the crack whereas mechanical inertial effects tend to limit the rate of crack extension, the crack speed stabilizes at approximately $å_{mb} = 0.6\ c_r$, which is the macroscopic crack branching speed for RT-PMMA.

EXPERIMENTAL SYSTEM

The experimental system (Fig. 1, left) was designed to enable a steady state regime of brittle fracture and a simple mechanical analysis of the fracture energy, even for RCP [2, 3]. The geometry is that of a strip band specimen (SBS) of typical dimensions $L \approx 200$ mm, $25 \text{ mm} < H < 45$ mm, $a_0 \approx 3\,H$, $B \approx 2$ mm. The location of the crack tip during propagation is determined by measuring the resistance of a metallic layer at a sampling rate of 250 kHz [4]. A loading device (Fig. 1, right) ensures uniform and constant displacement of the strip band boundaries and the symmetry of the loading is checked by strain measurements on the sides of the specimen.Crack propagation is started by an impact of low energy on a razor blade placed in contact with an initial blunt notch and the crack propagates symmetrically. Only one of the twin specimens undergoes fracture. Owing to the weight of the grips and the short fracture time, typically 200 μs, we assume that the boundary conditions are fixed during crack propagation. Crack branching can be obtained by increasing the mechanical potential energy of the specimen and the crack branches are generally symmetrical for polymethylmethacrylate (PMMA) and RT-PMMA specimens. RT-PMMA is a blend of PMMA and spherical rubber particles, in these experiments of diameter 200 nm and volume fraction approximately 40 %.

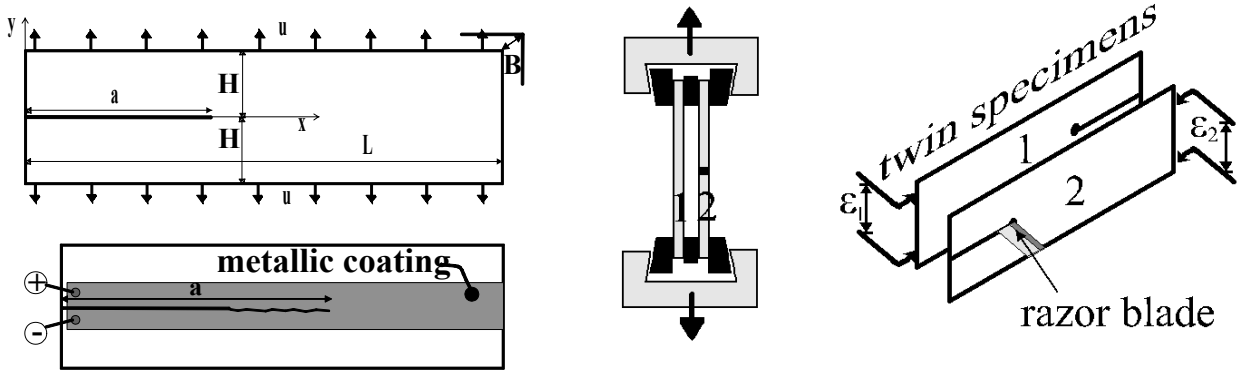

Figure 1: (left) Schematic representation of the strip band geometry uniformly loaded and the conducting layer used to record the crack tip position during propagation. (right) Experimental device ensuring symmetrical loading.

DYNAMIC ENERGY RELEASE RATE COMPUTATION AND VALUES OF THE FRACTURE SURFACE ENERGY

During RCP tests, no significant variation of the macroscopic crack speed has been observed for a given specimen at a given temperature, whether branching occurs or not (Fig. 2). Since the crack tip position during propagation and the stress state at initiation are known, the energy release rate G_{ID} may be calculated by means of a transient dynamic finite element procedure, using the software Castem2000©. Outside the singularity, thermo elastic effects are expected to be negligible since the mean stress is about 15 MPa [5]. Owing to the high strain rate, the fracture mechanics is assumed to display linear elastic behaviour [6]. The energy release rates were computed by differentiating the elastic energy integrated on the whole structure. As the geometry ensures a quasi-steady state regime of propagation, it is assumed that a specific treatment of the singularity is not necessary since the error done concerning the energy integration at the crack-tip singularity is eliminated by the differentiation. It has been shown experimentally that the impact on the razor blade influences the crack propagation only over the first few millimetres. Nevertheless, this crack initiation is simulated by imposing an initial crack tip opening, corresponding to the action of the razor blade at the crack lips.

Figure 3 shows that the dynamic correction factor is generally of the order of 0.7 to 0.8 for macroscopic crack speeds of about $0.6\,c_r$. This specimen geometry in fact induces a low dynamic correction factor [3, 7] and the remote stress field at the crack tip is not strongly influenced by inertial effects in this range of crack speeds. To simplify the results, as G_{ID} displays relatively small

oscillations during crack propagation, the mean value of the fracture energy $< G_{ID} >$ was calculated for each specimen before branching, if any. In practice, $< G_{ID} >$ concerns the steady state regime and does not take into account the first 1.5 mm of propagation in RT-PMMA. $< G_{ID} >$ varies from 0.49 to 2.1 KJ/m² and for a single straight line crack with smooth crack surfaces is typically 0.57 ± 0.12 KJ/m². In the case of a single straight line crack with crack surfaces showing small aborted but visible branches of length less than about 1 mm (Photo1), $< G_{ID} >$ is typically 0.8 ± 0.15 KJ/m². When macroscopic crack branching occurs, the crack surfaces are very rough before branching and $< G_{ID} >$ is of the order of 1.45 ± 0.7 KJ/m². The experimental mean dynamic fracture surface energy $< G_{ID} >$ for a crack propagating at several hundred metres per second is substantially lower than the fracture energy G_{Ic} at the onset of propagation, which is typically close to 10 kJ/m^2 at low or medium stress intensity loading rates. The crack speed is not correlated with $< G_{ID} >$ and lies in the range 550-610 m/s at temperatures between 19 °C and 27 °C.

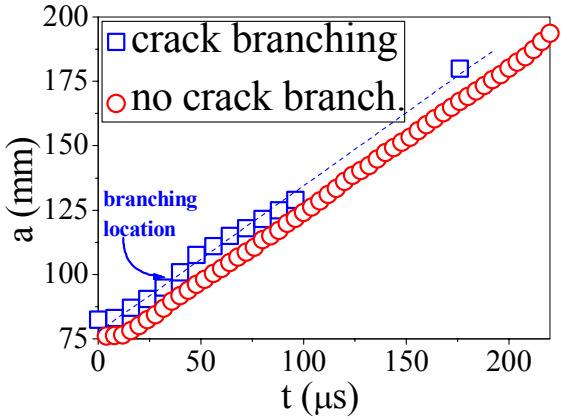

Figure 2: Crack length vs. time in the presence of crack branching (double branch at a = 99 mm) and in the absence of macroscopic crack branching. Note the similarity of the crack speeds and the quasi absence of crack speed variation.

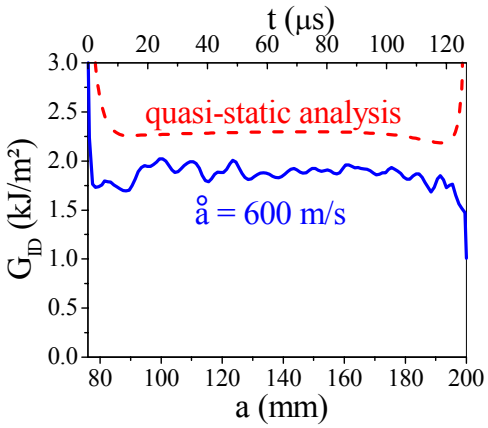

Figure 3: Quasi-static and transient dynamic finite element analyses: typical results for crack propagation without branching.

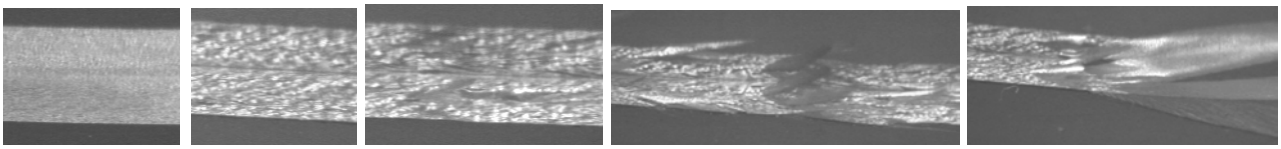

Photo 1: Photos showing different sizes of the frustrated micro-branches, increasing from left to right and corresponding to a RCP at about 0.6 c_r in an RT-PMMA. The cracks propagated from left to right. The entire specimen thickness, 2 mm, is visible and reflected on the metallic coating which acts as a mirror. The right hand photo shows a macroscopic crack branching (three branches) and a sudden change in the fracture surface roughnesses.

FRACTURE SURFACE ROUGHNESS

The fracture surface roughness displays a sharp change at branching, visible in the left and right parts of Photo 2. Optical microscopy reveals here a relatively coarse surface texture a few millimetres before branching (left) and a finer texture after branching (right). Figure 4 shows atomic force microscopy images of a fracture surface (left) a few millimetres before macroscopic crack branching, which corresponds to a high fracture surface energy and (right) just before crack arrest, which corresponds to the lowest fracture surface energy. It can be seen that also on a microscopic scale the surfaces are rougher prior to crack branching than before arrest at a similar crack speed. One notes further that the fracture surface does not pass through the rubber particles of RT-PMMA.

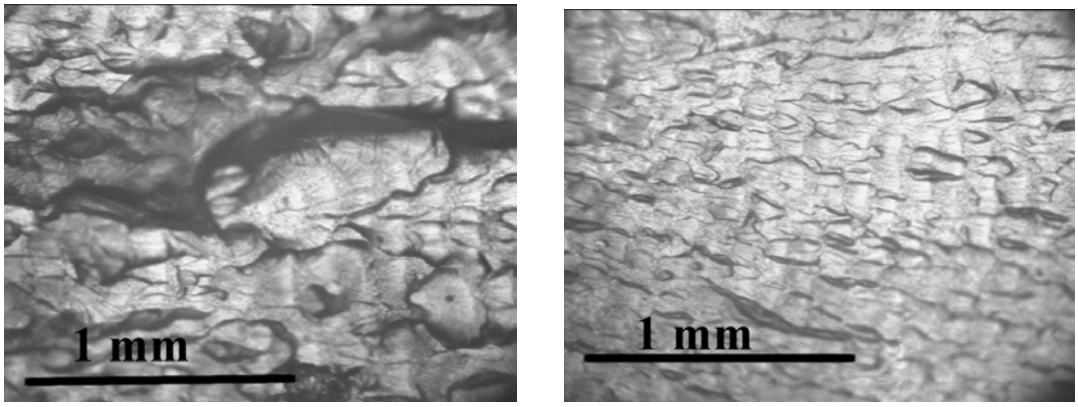

Photo 2: Optical micrographs showing the roughness change at branching: propagation from left to right in an RT-PMMA specimen of thickness 2 mm, (left) 9 mm before the onset of crack branching and (right) 7 mm after crack branching.

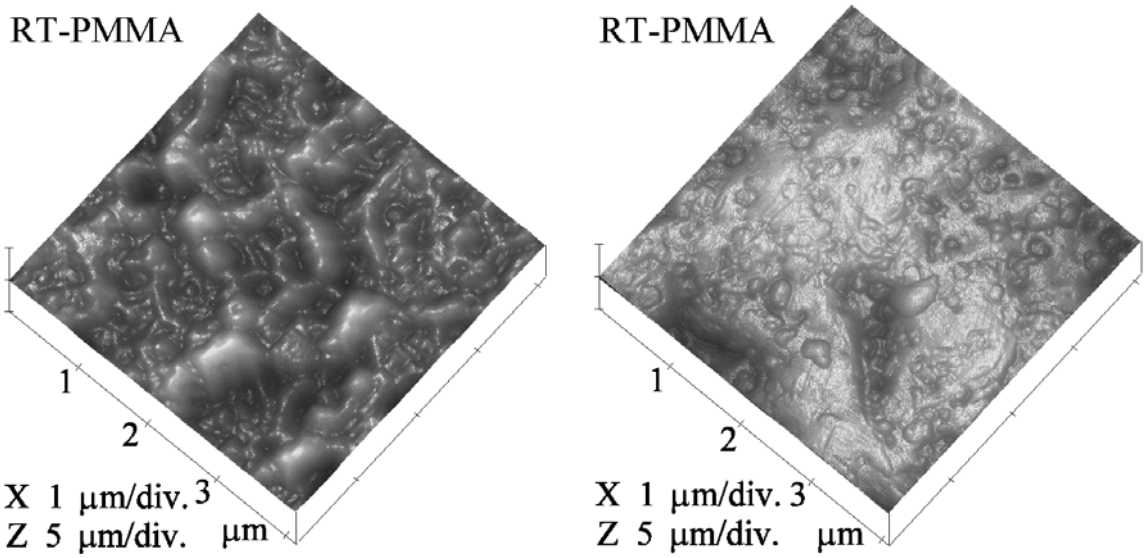

Figure 4: Atomic force microscopy images of a fracture surface: (left) rough surface before crack branching, åm > 500 m/s, and (right) smooth surface just before crack arrest, åm > 500 m/s.

Since the crack forms branches even though the experimental crack speed and the energy released inside the specimen remain quasi constant, two or sometimes three branches must consume the same energy as a single crack propagating at the same speed. The variable parameter at crack branching is thus the roughness of the fracture surface, which means the total surface created (S_{Ft}). As this may be approximately the same for two smooth crack branches as for a master rough crack, the usual planar crack surface (crack length increase multiplied by width, B Δa) cannot be employed. In the case of a smooth crack created at speed $å_{mb}$, as in Figure 4 (right), the fracture energy is G_{IDmin}. If the energy release rate is greater than G_{IDmin}, the propagating crack may produce microscopic instabilities since the inertial effects are sufficient to allow crack branching. These small instabilities are themselves

smooth and frustrated micro-branches. If the energy release rate exceeds twice G_{IDmin}, then two macroscopic smooth branches may appear. SBS fracture tests were also performed using pure PMMA specimens. In these samples, optical microscopy revealed mirror like fracture surfaces, while as expected [8, 9] the experimental fracture energy increased with crack speed. Figure 5 shows that G_{IDmin} is similar for PMMA and RT-PMMA at the equivalent crack speed. The fracture energy of RT-PMMA at a crack speed of $å_{mb}$ varies from 1 to 4 times G_{IDmin}, which corresponds to smooth crack surfaces, and we sometimes observed triple branching. Hence the fracture energy might be expected to be directly correlated with the ratio S_{Ft} / (B Δa) and the fracture energy of pure PMMA.

CONCLUSION

RT-PMMA represents an interesting model material to study the micro mechanisms of dynamic fracture processes. The present work shows experimentally and explains why the measured fracture surface energy has no single value at the macroscopic branching velocity, at least in materials in which the fracture energy decreases during RCP.

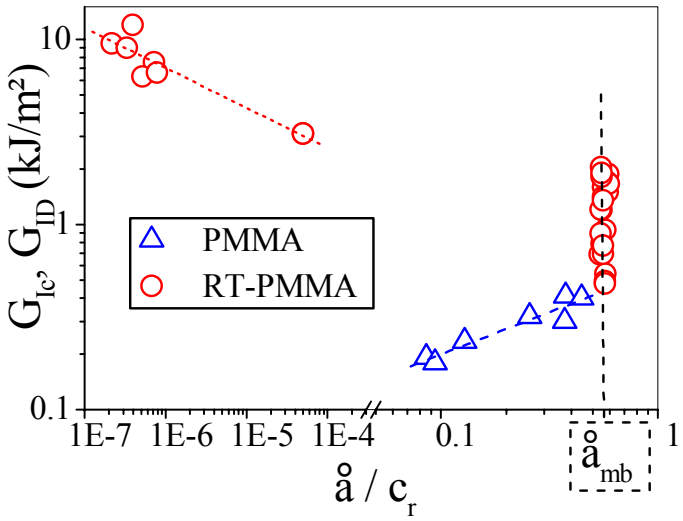

Figure 5: Fracture surface energy vs. normalized crack speed for PMMA and RT-PMMA.

REFERENCES

1. Yoffé, E. H., *Phil. Mag.*, **12**, (1951), p 739-750.
2. Fond, C. and Schirrer, R, *Journal de Physique IV*, (1997), p. C3-969-C3-974.
3. Nilsson, F, *Int. J. Fract. Mech.* **8**, (1972), p.403-411.
4. Thesken, J. C, The Aeronautical Research Institute of Sweden, FFA-TN, **57**, (1994).
5. Rittel, D., *Int. J. Solids Structures*, **35**, 22, (1998), p. 2959-2973.
6. Ferrer, J. B., Fond, C., Arakawa, K., Takahashi, K., Béguelin, P. and Kausch., H.-H., *Letters in Fract. and Micromech.* **87,** (1998), L77-L82.
7. Popelar, C. H. et Atkinson, C., *J. Mech. Phys. Solids*, **28**, 14, (1980), p. 77-93.
8. Williams, J. G., *Int. J. Fract.* **8**, (1972), p. 393-401.
9. Carlsson, J., Dahlberg, L. and Nilsson, F., *Proc. Int. Conf. Dyn. Crack Propag.*, (1972), ed. 1973, p. 165-181.